A Module-Based Plug-n-Play Dc Microgrid with Fully Decentralized Control for IEEE Empower a Billion Lives Competition

Dong Li, *Student Member, IEEE*, Carl Ngai Man Ho, *Senior Member, IEEE*

Abstract—In this paper, a module-based plug-n-play (PnP) dc microgrid is introduced to help rural electrification. It provides a bottom-up way to form a microgrid (MG) with multilayer expandability and Plug-n-Play feature. The module-based MG overcomes the drawback of conventional MG that requires central design and implementation which leads to high upfront cost and long lead time. It provides an organic way to form a MG that allows user to scale up the system as their demands growing, and fully utilize the existing resources. The proposed MG module is expandable on different layers that can meet requirements of customers with different power consumption requirements. Each module, which contains PV generation and energy storage, can work as a standalone solar home system. Multiple modules can be connected as a group to scale up the local power supply. Groups can be interconnected through a public bus with gateway converter modules to form a community network, which can supply public usages and enables power exchange in a community range with relatively high distribution efficiency. The control of proposed MG is in a fully decentralized manner, that central control and communication network can be omitted, which makes the system more user-friendly and highly robust. Detailed design, analysis and implementation of the proposed PnP MG is provided in this paper. Simulation and experimental results have been provided to verify the concept and analytical study.

Keywords—*dc microgrid, modular microgrid, microgrid module, decentralized control, rural electrification*

LIST OF ABBREVIATIONS

BES   Battery Energy Storage
GC   Gateway Converter
MG   Microgrid
MPP   Maximum Power Point
MPPT   Maximum Power Point Tracking
PnP   Plug-and-Play
PU   Power Unit
PV   Photovoltaic
SHS   Solar Home System
SoC   State of Charge

I. INTRODUCTION

According to International Energy Agency, over 3 billion people are living in energy poverty and more than 1 billion people are living with no access to electricity [1]. It has been a challenge to develop new ways to power up these unelectrified areas. The high cost and geographical limitations in most of unelectrified areas make the conventional power system, which
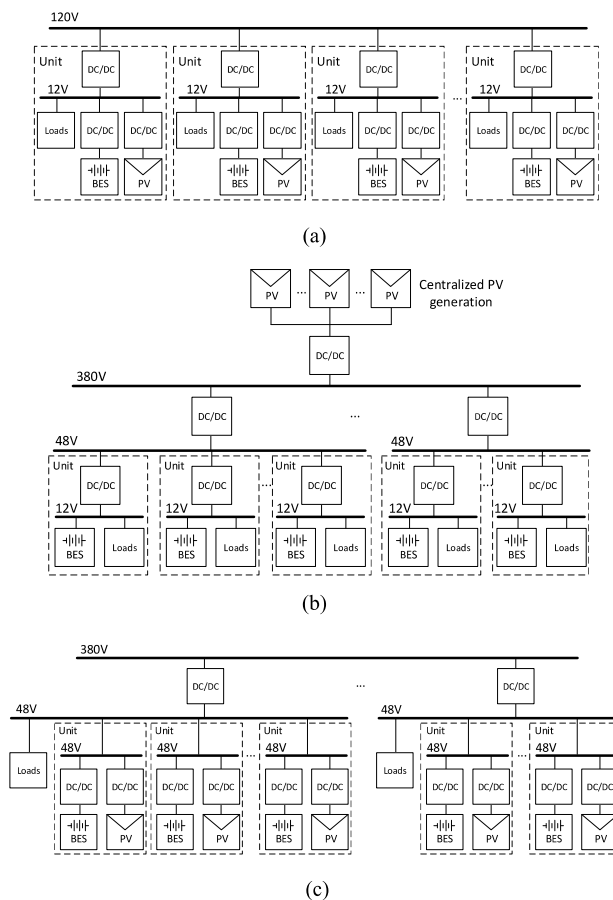

Fig. 1. Prior-art and proposed scalable microgrid structures, (a) scalable microgrid structure used in [14]-[16], [18], (b) scalable microgrid structure proposed in [17], (c) PnP microgrid proposed by this paper.

relies on central generation and long-distance transmission, no longer effective to solve the current energy poverty problem [2]-[3]. Meanwhile, to power up billions of people with conventional fuel-burn plants could generate giga tons more of carbon emission. Alternatively, Photovoltaic (PV) based off-grid dc microgrid systems have been developed with new business models to make electricity affordable to households in energy poverty areas [2].

Most of the less-electrified regions are in Africa and South Asia where is rich of solar resources. This makes solar photovoltaic generation a competitive way towards conventional generation. The distributed character of PV

generation relies on microgrid (MG) as an effective way to utilize solar energy [4]-[7]. MG integrates generation, load and energy storage, which can constantly provide relatively high power and support a variety of loads. However, the common approach to build a MG requires a centralized design, installation and operation. As a result of this top-down approach, professionals are required, the cost (including design, installation and operating) are increased, the lead time is prolonged, and the future expansion of MG is difficult. With conventional approach, the MG capacity will be overdesigned or insufficient in most of time due to the difficulty of expanding. And it is hard for people living in energy poverty to raise money for the upfront investment. These drawbacks are strangling development of MG in rural areas.

To overcome the drawbacks of conventional central MG by making MG plug-and-play (PnP) to be easily scaled up, more and more researches on flexible MG structures, modular MGs and MG clusters have been proposed [8]-[12]. Paper [13] have pointed out few major concerns to achieve PnP in MG system, among which the most important is how to avoid communication which may spoil the scalability and reduce system reliability and how to design a decentralized control system independent from total number of modules to achieve a real scalable design. Paper [14]-[15] studied distributed control technologies based on peer-to-peer communication. [14] proposed an Open Energy System that allows independent nanogrids being interconnected as a microgrid, which relies on a peer-to-peer control system. Similarly, paper [15] proposed a distributed cooperative control system. Though the central controller is eliminated, the systems still highly rely on communication network, which may not be preferred in a rural application that communication could increase cost and reduce reliability as well as the scalability. Paper [16]-[18] provided decentralized solutions that the MG system can become independent from communication and realize PnP. Paper [16] proposed a scalable MG architecture based on droop control that only relies on local information which is highly suitable for rural electrification. Paper [17] proposed a scalable MG with centralized generation and decentralized home power management units (PMUs). Paper [18] proposed a Self-Organizing NanoGrid (SONG) system, which is based on a low-cost multiport converter unit.

Fig. 1 (a) shows a typical structure of scalable MG. Most of prior arts of scalable microgrid are based on this general structure, where the control, topology and scale may vary in different projects. The expansion is based on a dc-dc converter as an interface of each unit. The advantage of this structure is simple control that each unit is isolated by the interfacing dc-dc converter and just needs to manage power balance of its own. However, the disadvantage is also obvious. Firstly, since the house load is connected to local bus, the available power to the load is limited by the rating of interfacing dc/dc converter regardless of number of units. Secondly, when power goes from one unit to another unit, it needs to go through interfacing converter two times, which could be lossy.

Fig. 1 (b) shows the scalable microgrid structure used in paper [12]. Instead of having PV modules in each unit, this structure has a centralized PV generation. The Power Management Units (PMU) installed at each user only contains BES and loads. Thus, the control of each unit can be significantly simplified without local generation. The available power on the 12V bus is also limited by the single converter capacity. Power on the 48V cluster bus is scalable. However, due to the centralized generation, the modularity is reduced that a single unit cannot work without generation, and it is economic viable only for relatively large communities.

Fig. 1 (c) shows the proposed PnP microgrid structure. Firstly, in this structure, each unit has BES and PV generation which can be used as a standalone unit. Secondly, since the connection of multiple units uses local bus directly without any interfacing converters, the power on the 48V bus is scalable without single converter limit and the loss is reduced without interfacing converters. Thirdly, to interconnect multiple groups, an interface converter, or called a gateway converter, is used to create a relatively high voltage distribution network.

As shown in Fig. 1 (c), the proposed MG has three expansion layers. Firstly, a single power unit (PU), can work as a standalone SHS. Each PU contains PV generation and BES with a common 48V dc bus as output. Secondly, multiple PUs can be interconnected directly with the 48V local dc bus as a group. Thirdly, multiple groups can be connected to a public dc link (200V-400V), through gateway converters. Inter-group expansion is at community level and allows power exchange among households and pooling power for public usages.

Conventionally, for central-planned commercial dc microgrid, communication-based hierarchical control structure is commonly used [19]-[21]. The involvement of control center and communication network significantly reduces system modularity. To better introduce PnP into microgrid, the study on decentralized control become popular. Literatures [14]-[15] and [22]-[24] studied decentralized control of microgrid. Though the central controller is removed, they still rely on communication network. Most of studies on communication-less control of microgrid only focus on primary control and system stability [25]-[27], while some other important aspects of microgrid control, e.g. State-of-Charge (SoC) balancing, control mode selection, are overlooked. In this paper, to keep a high modularity and reliability, a fully decentralized and communication-less control is applied to the proposed MG system. The direct bus connection inside a group increases the difficulty of coordinating all the parallel Battery Energy Storage (BES) converters and parallel PV converters. It is challenging to achieve power sharing, BES SoC balancing, PV-BES coordination, and inter-group coordination at the same time in a communication-less manner. The proposed control is based on modified droop control, of which the stability is as good as common droop-controlled systems. With proposed control methods, units can be bus interfaced with a well-designed droop control system based on dc bus signaling technology [28]-[29].

Control for each PU is fully decentralized and does not need any modification in different expansion levels and operation modes. Grid-connection is possible when a grid is available.

The proposed MG solution has advantages of,

1) It allows a bottom-up way to establish a power network. Users can start with single PU and expand the system as their demand and budget growing or interconnect the system with their neighbors'.
2) Separate local household-level bus and public dc bus allows using of two voltage levels. The low voltage 48V household-level bus is safe for untrained people to use and install. High voltage public bus keeps low distribution loss.
3) Public dc bus is isolated from each local dc bus with GCs. Reliability is improved that failure can be isolated within the local bus range.
4) Group expansion can be achieved without interfacing converters, which reduces cost and power loss.
5) The modular design of PU and gateway converter could significantly reduce the design cost of MG and enables mass production.
6) Fully decentralized control keeps high reliability and robustness, saves cost on communication devices.

Noticing that all PUs in one group share only one common bus, a relay is necessary at each PU's output terminal to protect devices under fault condition. And the number of PUs connected to one local bus should be limited to a reasonable value not exceeding GC capacity and to guarantee a good reliability.

The proposed MG has a bottom-up building feature that allows system growing organically as the demands growing. The feature that combines advantages of conventional SHS and central MG could significantly reduce the difficulty of developing MGs in rural developing areas.

The paper is organized as follows: In section II, the architecture of proposed module-based MG is introduced. In section III, detailed design of fully decentralized MG control is provided. Section IV provides simulation and experiment results to verify the analytical study. Conclusion is given in Section V.

II. ARCHITECTURE OF PROPOSED PnP MICROGRID

As shown in Fig. 1 (c), the proposed PnP MG has three expansion levels, standalone, group expansion and inter-group expansion. This section will introduce the proposed MG architecture by these three expansion levels.

In standalone mode, a single PU can operate as a SHS, providing basic energy supply. Fig. 2 shows the diagram of a single proposed PU. The PU consists of two power electronic converters, a dc-dc converter for PV generation and a dc-dc converter for BES. Each PU is controlled by an independent digital controller.

Multiple PUs can be interconnected directly through the local dc link to provide bulk power to users as a group. Fig. 3 shows the diagram of a MG contains multiple groups. As mentioned in the introduction, direct bus-interfacing could omit interfacing converters, however the control coordination could become challenging, which will be discussed in detail in Section III.

Multiple groups can be interconnected to a public network in a relatively large area to enable power exchange among households and usage of public loads. Fig. 3 shows the diagram of proposed MG in inter-group expansion. The interconnection of groups requires interfacing converters called as Gateway Converters (GC) in this paper. The GC boosts the low voltage (48V) on the group side to a high voltage (200V-400V) on the
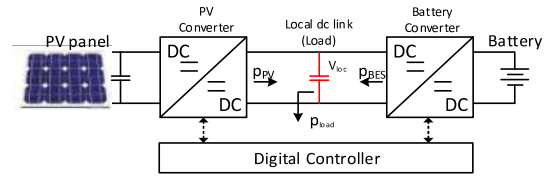

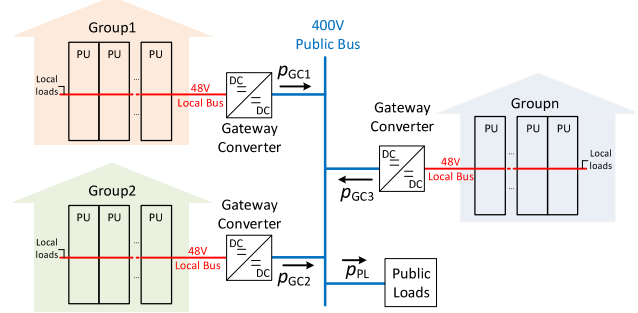Fig. 2. Diagram of a proposed power unit (PU).

Fig. 3. Diagram of proposed MG with inter-group expansion.

public network side, provides galvanic isolation, and controls power flow between local group and the public network. With proposed control method, GC could compensate net load/generation differences and balance SoCs among groups automatically without communication.

Notice that, the PUs inside a group are very close to each other, where the line resistance among the PUs can be obviously neglected. For the public network, the line resistance can also be neglected to simplify the study considering two facts:

i. The community network is still in a relatively small scale (in a hundreds-meters range). With proper selection of conductor size and voltage level, the line resistance is very small.
ii. Each GC only maintains bus voltage at its terminal with droop control, the line resistance only affects the performance of power sharing among groups. The virtual resistance in droop control is much larger than line resistance. Thus, the effect of line resistance on power sharing is also neglectable.

III. DECENTRALIZED CONTROL STRATEGY FOR PROPOSED MICROGRID MODULE

To achieve PnP and robust operating in all expansion levels while keeping low cost and high reliability, a fully decentralized control system independent from communication has been designed in this paper. Mode transitions of each converter can be achieved seamlessly. The proposed method is developed from dc bus signaling control proposed by [28]-[29]. And new SoC self-convergence control and seamless PV mode adaptive control are integrated to the conventional dc bus signaling technology. This section introduces the detailed design and implementation of proposed decentralized control to achieve proposed scalable MG in a wireless and seamless manner.

A. BES Converter Control

In a regular operation scenario, the BES converter should regulate local dc bus voltage with droop control to compensate the power mismatch between PV MPPT output and load consumption. Besides voltage regulation, the BES SoCs of
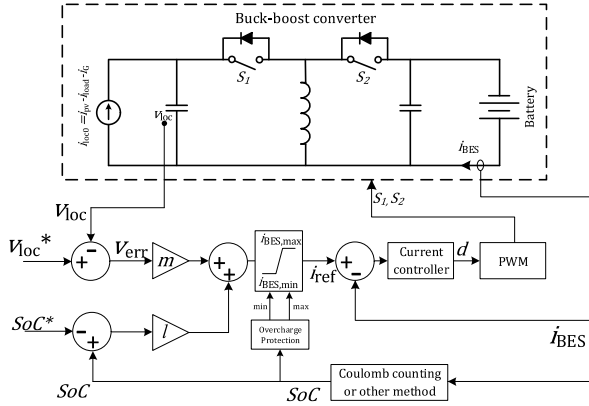
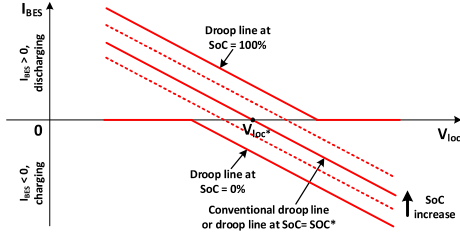Fig. 4. Block diagram of SoC-based droop control for BES converter.

Fig. 5. Droop lines of SoC-based droop control under different SoCs.

parallel PUs should be kept balanced to make full usage of each battery. Paper [30] and [31] have proposed modified droop control to achieve BES SoC self-convergence without communication, by adjusting the droop resistance. Different from existing solutions, to accommodate dc bus signaling, this paper adds a first order term to the conventional droop control to achieve SoC self-convergence, rather than changing the droop resistance, which is important for the control coordination in the proposed MG. Fig. 4 shows the diagram of proposed controller for BES converter. The modified droop control, which is based on I-V droop control, follows,

$$i_{BES} = m_{BES}\left(V_{loc}^* - v_{loc}\right) + l\left(SoC - SoC^*\right) \qquad (1)$$

where V_{loc}^* is the rated local bus dc link voltage and SoC^* is a reference value of SoC ramp term.

Fig. 5 shows droop lines of proposed modified BES droop control. Besides the conventional I-V droop term that output current is proportional to voltage error, it contains a SoC ramp term. With the additional term, the output current will slightly increase when BES SoC level is higher than SoC^*; the output current will slightly decrease when SoC level is lower than SoC^*. Thus, an SoC self-convergence characteristic can be created. By properly selecting parameter l, the voltage deviation can be kept in an acceptable range.

It is also shown in Fig. 4, a saturator is added to the BES current reference. A overcharge protector provides limits for saturation stage based on information of SoC. When SoC is 0% or lower than a minimum SoC level, the current upper limit is set to zero (prevent from over-discharging); when SoC is 100%, the current lower limit is set to zero (prevent from over-charging). When the BES operating is limited by the saturator, the BES converter lost the droop characteristic. At this point, the bus voltage should be maintained by PV converter(s) (when
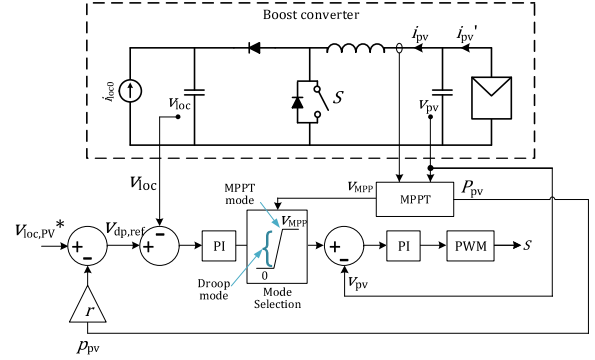

Fig. 6. Block diagram of PV converter control with seamless mode selection.

BES is saturated to charging limit) or gateway converter (when BES is saturated to discharging limit).

The proposed MG has to use proposed SoC self-convergence control with a first-order SoC term rather than conventional method as discussed in [30] & [31], due to the following reasons,

i. Some other important control parameters are selected based on the BES droop coefficient m_{BES}. The proposed method has a fixed droop coefficient rather than the conventional method adjusting droop coefficient all the time.

ii. Another important reason is the linearity, which the conventional method cannot provide. Proposed method provides a linear relationship between local voltage, local SoC, and local net generation/load, which will be used for the GC control to compensate the power mismatch and SoC unbalance among multiple groups.

iii. The proposed method also takes advantage of consistency in charging and discharging process and stable balancing speed, which is not related to charge/discharge power.

Under BES droop control, v_{loc} follows,

$$v_{loc} = V_{loc}^* + \frac{l}{m_{BES}}\left(SoC - SoC^*\right) - \frac{1}{m_{BES}}i_{BES} \qquad (2)$$

which is used in the dc bus signaling system design.

B. PV Converter Control

In a grid-connected PV system, PV panels can always operate under MPPT control theoretically while the grid can always absorb surplus power. However, in a small off-grid system as proposed MG, PV generation has to be able to operate under droop control when BES is fully charged. Paper [32] proposed a control for PV sources with a switch choosing two control configurations, which increase system complexity. Paper [33] proposed a seamless control for PV sources with an inner control loop to control dP/dV, which can achieve seamless mode transition by a saturator to dP/dV reference. However accurate measurement of dP/dV could be difficult especially for a low-cost application for rural electrification. This paper proposed an alternate PV controller with seamless mode transition and more practical implementation. Fig. 6 shows the proposed mode adaptive PV converter control diagram. The inner control loop is a PV voltage loop maintains PV panel voltage. The outer control loop is a V-I droop control loop that maintains local dc link voltage, with a higher voltage reference value compared to BES droop control. The mode transition is seamless that the saturator and local bus voltage PI controller provides the ability of automatic mode transition.
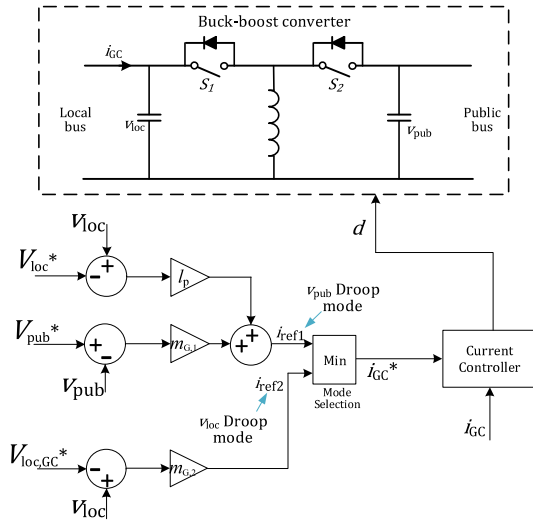
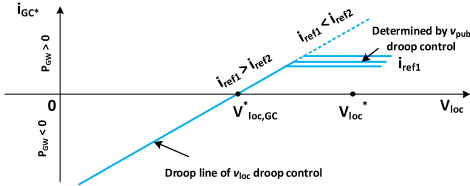Fig. 7. Block diagram of gateway converter control.

Fig. 8. Droop line of local bus droop control of gateway converter.

When the BES is not yet fully charged that the local dc link voltage is well regulated by BES converter, $V_{dp,ref}$ is always higher than v_{loc}, with a preselection of $V_{loc,PV}^*$. The input of voltage PI controller is constantly positive, so the output of PI controller is saturated to higher limit which is set to MPP voltage. The inner loop will control v_{PV} to V_{MPP} which achieves MPPT.

When PUs are fully charged or the BES current already hit the limit of $i_{BES,min}$ (maximum charging current), the local dc link voltage will rise higher than $V_{dp,ref}$. Then the V_{PV} reference will decrease lower than V_{MPP}, so PV may operate at an off-MPP mode. Under PV droop control, v_{loc} follows,

$$v_{loc} = V_{loc,PV}^* - r \cdot p_{PV} \qquad (3)$$

When load increases that $p_{PV} < p_{load}$, the dc link voltage will drop, V_{PV} will rise up until reaching MPP and BES starts to discharge and maintains local dc link voltage.

C. Gateway Converter Control

Fig. 7 shows the control diagram of GC in proposed MG architecture. Any bidirectional dc-dc topology can be used for GC, e.g. Boost, Flyback, Forward, Dual-Active-Bridge, etc. And in this paper, Buck-Boost converter is used for GC to demonstrate the general idea. As the interface between local low-voltage dc bus and public medium voltage dc bus, the gateway converter has two operation modes, v_{pub} control mode and v_{loc} control mode. Similar to PV mode selection, which is based on a voltage threshold, the gateway converter mode selection uses smaller current reference from i_{ref1} (generated by

public bus droop control) and i_{ref2} (generated by local bus droop control). As a result, the power direction change becomes continuous and seamless. Gateway converter and BES converter can work simultaneously under droop control establishing local dc bus voltage.

In v_{pub} control mode, the local group operating in healthy condition, the gateway converter will maintain the public dc bus voltage with a modified droop control, as $i_{ref1} < i_{ref2}$ in Fig. 7. The current reference in v_{pub} control mode is given by,

$$i_{ref1} = m_{G,1}\left(V_{pub}^* - v_{pub}\right) + l_p\left(v_{loc} - V_{loc}^*\right) \qquad (4)$$

In v_{loc} control mode, the energy stress of the local group is too high to support public network that $i_{ref2} < i_{ref1}$, the GC can reduce output power even to reversely inject power into the local group to maintain the local dc link voltage inside acceptable level. The controller for gateway converter in v_{loc} control mode uses simple I-V droop control,

$$i_{ref2} = m_{G,2}\left(v_{loc} - V_{loc,GC}^*\right) \qquad (5)$$

where $V_{loc,GC}^*$ is rated voltage for GC local bus droop control. The selection of $V_{loc,GC}^*$ will be detailly explained in Section III D.

The mode selection is based on i_{ref2}, which is actually an indicator of group energy stress. The larger i_{ref2} is, the less stressed the group is. In v_{pub} control mode, $i_{ref2} > i_{ref1}$, the gateway converter will follow the public bus droop control. In v_{loc} control mode, $i_{ref2} < i_{ref1}$, the gateway converter will maintain the local dc bus at a minimum level. Fig. 8 shows the droop line of local bus droop control of gateway converter.

For selecting parameters of GC control, an important difference is GC could be connected to groups with different number of PUs. Thus, the control parameters of GC should be adjusted according to the number of PUs connected to local group to proportionally share power with other groups. The setting of number n can be achieved by simply using buttons or a knob on the GC, which can be done by any untrained people and will not spoil the PnP feature. Thus, $m_{G,2}$, $m_{G,1}$ and l_p should be adjusted accordingly,

$$m_{G,1} = n \cdot m_{G,1}' \qquad (6)$$
$$m_{G,2} = n \cdot m_{G,2}' \qquad (7)$$
$$l_p = n \cdot l_p' \qquad (8)$$

where n is the number of PUs connected to the local bus, $m_{G,1}'$ and $m_{G,2}'$ are droop coefficients per unit for local bus droop control and public bus droop control, respectively, l_p' is the per unit coefficient for SoC balance among groups.

The values of $m_{G,1}'$ and $m_{G,2}'$ could follow regular droop controller design procedure considering the acceptable range of voltage variation towards certain power variation. Specifically, to achieve same voltage regulation performance on local bus under usage-dominating mode as under storage-dominating mode, $m_{G,2}'$ should be equal to m_{BES}. l_p' should also be equal to m_{BES} to achieve automatic compensation of load/generation mismatch, which will be explained later.

Different from conventional solutions as shown in Fig. 1 (a) where the interfacing converter, BES converter and PV converter can be controlled by one controller device with shared information. A challenge for GC is how to achieve power flow

control and SoC balance among groups simultaneously without communicating with other devices. The proposed GC control coordinate with proposed BES droop control as introduced in Section III. A, naturally, which achieves automatic power flow control to compensate load/generation mismatch and SoC self-convergence among multiple groups.

As shown in equation (4), the GC v_{pub} droop control also consists of two terms, one conventional I-V droop control term and a first-order term reflects local voltage. Considering groups could have different numbers of PUs, equation (4) can be rewritten as,

$$\frac{i_{GC}}{n} = m'_{G,1}\left(V^*_{pub} - v_{pub}\right) + l'_p\left(v_{loc} - V^*_{loc}\right) \quad (9)$$

where i_{GC} is the current of the GC on the local bus side.

All GCs are connected to the same public bus, so the first terms in (9) are same in all GCs. Thus, the circulating current to balance power and SoC is only generated from the second term,

$$i_{GC,c,p.u.} = l'_p\left(v_{loc} - v_{loc,avg}\right) \quad (10)$$

where $i_{GC,c,p.u.}$ is the per PU circulating current go through GC converters. With local SoC self-convergence control proposed in section III A, the local bus voltage contains information of both group net load/generation and group average SoC. Put (2) into (10),

$$i_{GC,c,p.u.} = \frac{l'_p}{m_{BES}}\left(i_{BES,avg} - i_{BES}\right)$$
$$+ \frac{l'_p l}{m_{BES}}\left(SoC_{loc,avg} - SoC_{global,avg}\right) \quad (11)$$

Apparently, the circulating current as in (11) consists of two parts. The first term, $\frac{l'_p}{m_{BES}}\left(i_{BES,avg} - i_{BES}\right)$, is used to provide compensation for load/generation mismatch among the groups. When $\frac{l'_p}{m_{BES}} = 1$, the first term becomes exactly the current mismatch of each PU. The second term, $\frac{l'_p l}{m_{BES}}\left(SoC_{loc,avg} - SoC_{global,avg}\right)$, is used to balance the SoCs among multiple groups. Make the difference between $SoC_{loc,avg}$ and $SoC_{global,avg}$ to be $\Delta SoC_{loc,avg}$, which can be expressed follow the definition of SoC,

$$\frac{d\Delta SoC_{loc,avg}}{dt} = -i_{BES} + i_{BES,avg} \quad (12)$$

Put (11) into (12) and considering $\frac{l'_p}{m_{BES}} = 1$,

$$\frac{d\Delta SoC_{loc,avg}}{dt} = i_{GC,c,p.u.} - l\Delta SoC_{loc,avg} \quad (13)$$

Solve (13),

$$\Delta SoC_{loc,avg}(t) = \Delta SoC_{loc,avg}(0) + \frac{i_{GC,c,p.u.}}{l}\left(1 - e^{-lt}\right) \quad (14)$$

Thus the SoC difference can be converged to,

$$\Delta SoC_{loc,avg}(\infty) = \Delta SoC_{loc,avg}(0) + \frac{i_{GC,c,p.u.}}{l} \quad (15)$$

From (15) it can be seen, the SoC converge performance on GC converters is different from BES converters. It cannot guarantee SoC difference converging to zero but only to a certain value related to GC operating condition. Though the

SoCs among groups will have difference, the trend is kept from divergence. This difference is caused by different load/generation conditions in multiple groups. Only when the net load/generation per PU of all groups are equal, $\Delta SoC_{loc,avg}(\infty)$ is equal to zero. Considering the per unit net load/generation in each group would be similar in a large time scale, the SoCs among groups can be kept balanced in long term dynamically.

D. Control Coordination

As mentioned, for each group, multiple PUs are directly bus-interfaced. The coordination of parallel PV, BES and GC converters is the key challenge in proposed MG architecture. While the public dc bus control is much simple and have been studied by many researchers, this section will be more focused on the local group control coordination.

With proposed controllers for each converter, the coordination, including mode transition, power sharing and SoC balance can be achieved simultaneously in a fully decentralized manner. As introduced above, generally, each converter in the proposed MG generally has two operation modes, which can be concluded as Table I. All mode transitions are based on seamless control.

TABLE I.   SUMMARIZE OF CONVERTER MODES AND CRITERIAS

	Mode 1	Mode 2	Mode transition criteria
BES converter	v_{loc} droop control	saturated	SoC level
PV converter	MPPT	v_{loc} droop control	v_{PV} reference saturated to V_{MPP} or not
Gateway converter	v_{pub} droop control	v_{loc} droop control	Comparing i_{ref1} and i_{ref2}

Besides modes of each converter, the overall system operation can be put into three modes. Fig. 9 demonstrates the coordination of PV, BES and GC droop control. Based on which part is dominating droop control, the three modes are generation dominating mode, storage dominating mode and usage dominating mode [28]. The local dc link voltage v_{loc} works as an indicator of operation mode. To achieve wireless and seamless mode transition, the parameters for each converter controller should be carefully designed.

PV should operate under MPPT control whenever BES can maintain v_{loc}. By (2) and (3), the parameters should satisfy,

$$V^*_{loc,PV} - r \cdot p_{PV,max} \geq$$
$$V^*_{loc} + \frac{l}{m_{BES}}\left(SoC_{max} - SoC^*\right) - \frac{1}{m_{BES}}I_{BES,min} \quad (16)$$

And noticing that the power range of PV is dependent on MPP power, a voltage gap between PV-droop control and BES droop control is inevitable, which will not have any negative influence on the system stability or reliability.

Different from having a relatively clear boundary between PV dominating mode and storage dominating mode, the storage dominating mode can have an overlapping area with usage dominating mode. It is allowed to have v_{loc} under droop control simultaneously from BES and GC. This overlap can reduce the stress of local BES at low SoC level and make the mode transition process smoother. The overlap is generated naturally from the selection of parameter $V^*_{loc,GC}$. Reaching the local
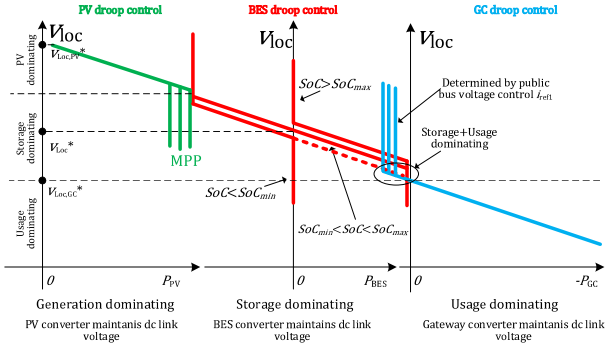
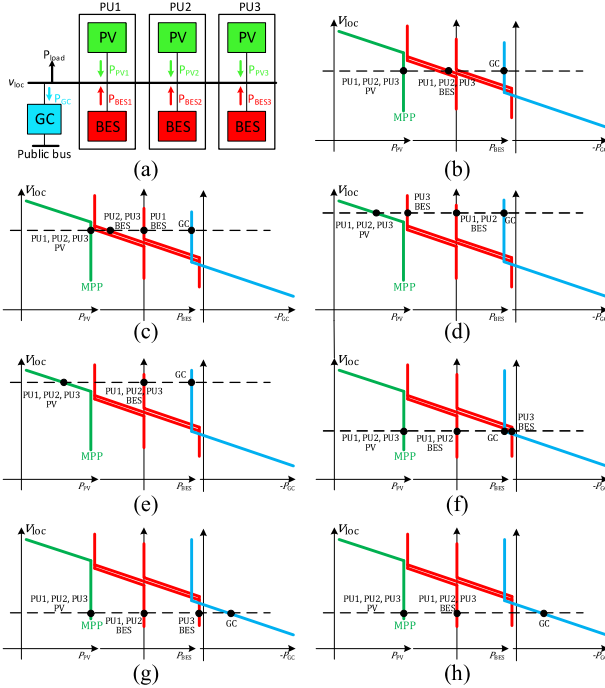Fig. 9. Coordination of local dc bus droop control.

TABLE II.   SIMULATION AND EXPERIMENT PARAMETERS

Item	Symbol	Value	Item	Symbol	Value
Rated local dc bus voltage	V_{loc}^*	48 V	Max discharging current	$i_{BES,max}$	4.2 A
Droop reference of PV converter	$V_{loc,PV}^*$	52 V	Max charging current	$i_{BES,min}$	-2.0 A
Droop reference of GC	$V_{loc,GC}^*$	44 V	BES v_{loc} droop coefficient	m_{BES}	1
Rated Public dc bus voltage	V_{pub}^*	200 V	BES SoC coefficient	l	0.02
BES voltage	V_{bat}	48 V	PV maximum power	$P_{PV,max}$	100 w
BES capacity	C_{bat}	10 Wh	PV droop coefficient	r	0.01
maximum SoC	SoC_{max}	100 %	GC v_{pub} droop coefficient	$m_{G,1}'$	0.1/unit
minimum SoC	SoC_{min}	30 %	GC v_{loc} droop coefficient	$m_{G,2}'$	1/unit
SoC^*	SoC^*	50 %	Group SoC coefficient	l_p	1/unit
Local bus capacitance	C_{loc}	660 μF/unit			

Fig. 10. Typical operating modes of a group in proposed MG, (a) group diagram, (b) storage dominating mode with all batteries available, (c) storage dominating mode (PU1 drained), (d) PV dominating mode (PU1&PU2 fully charged, PU3 at charging current limit), (e) PV dominating mode (all PUs fully charged), (f) storage dominating mode + usage dominating mode (PU1&PU2 drained), (g) Usage dominating mode (PU1&PU2 drained and PU3 at discharging current limit), (h) Usage dominating mode (all PUs drained).

voltage reaching $V_{loc,GC}^*$ means the BESs cannot further provide any power. Any further decrease of local bus voltage should be compensated by injecting power from GC. Thus, it makes sense to set GC power equal to zero at $V_{loc,GC}^*$ and $V_{loc,GC}^*$ should follow,

$$V_{loc,GC}^* = V_{loc}^* - \frac{1}{m_{BES}} I_{BES,max} \qquad (17)$$

The width of overlapping is determined by i_{refl}, which is generated from public bus voltage droop control.

Fig. 10 shows typical operating scenarios of a group consists of three PUs and one GC under different operation modes. Fig. 10 (a) shows the group connection diagram. Fig. 10 (b) shows a regular condition that all PUs are available, batteries can absorb or release energy to maintain the local bus voltage with droop

control, the system is under storage dominating mode. The operating points of three BES converters are on the droop line, three PV converters are under MPPT control and GC can be regard as load feeding power into public dc link. In Fig. 10 (c), though PU1 is fully charged that the operating point is saturated to zero current, the other PUs still can absorb surplus power, the group still operates under storage dominating mode. In Fig. 10 (d), PU1 and PU2 are fully charged and PU3 hits the maximum charging power, all PUs cannot further absorb surplus power. Thus v_{loc} rises and PV converters operates under droop control to maintain v_{loc}, which makes the system PV dominating mode. In Fig. 10 (e), all PUs are fully charged and the group is kept in PV dominating mode, until PV output cannot meet the load consumption, batteries will start to discharge and change back to storage dominating mode. In Fig. 10 (f), PU1 and PU2 BESs are drained and saturated to zero output power, though both PV are under MPPT control, v_{loc} is at a relatively low level due to the high load. GC operates under droop control with reduced power consumption. The system v_{loc} is dominated by both storage and usage. In Fig. 10 (g), PU1 and PU2 are still drained, and PU3 BES is saturated to its maximum output power, BES losses the ability of v_{loc} control. Only GC operates under droop control. The system is under usage dominating mode. Fig. 10 (h) is similar to Fig. 10 (g), but with all PU BESs drained. GC operates under droop control. The system is still under usage dominating mode.

With the proposed control system design, with a certain v_{loc}, a unique operating point can be determined for each converter in the group. In all operating scenarios and expansion levels, the system can be kept stable and robust. Therefore, a true PnP feature can be realized with low cost and high reliability.

IV. SIMULATION AND EXPERIMENTAL STUDY

A. Simulation Study

Simulations based on PLECS are performed to evaluate the proposed MG architecture and the fully decentralized control technique. Table II shows parameters used in simulation.

Fig. 11 shows the simulation results of a group consists of three PUs, where (a) shows the whole scope and (b)-(e) show the zoomed in waveforms during transients. In $t_0 - t_1$, all BESs of three PUs are under droop control and all PVs are under MPPT control (with different MPP power). At t_1, BES of PU1

(a)

(b)   (c)
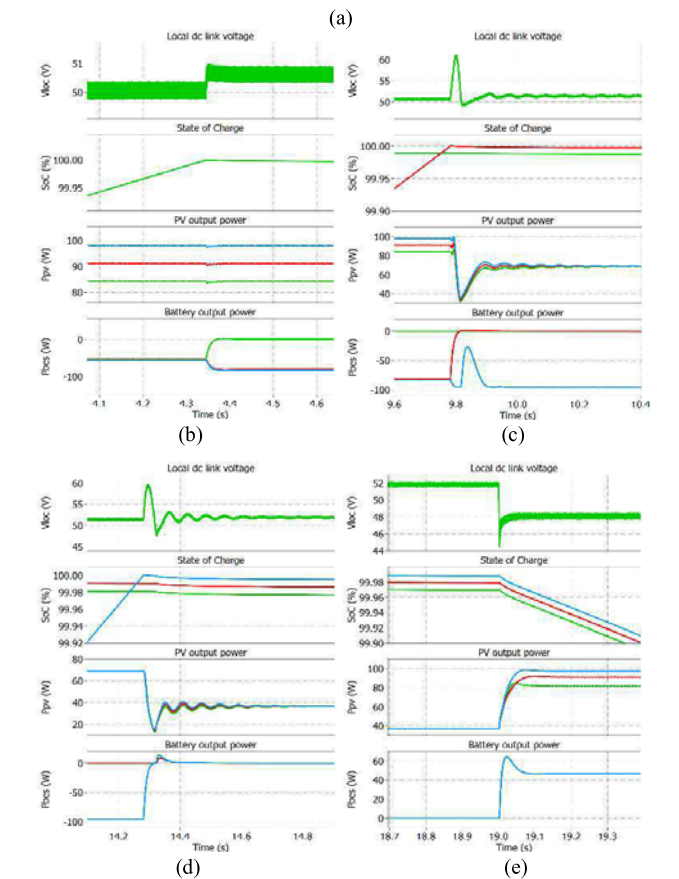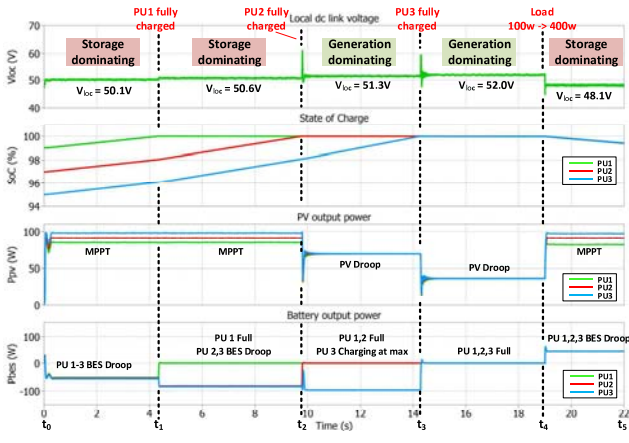

(d)   (e)

Fig. 11. Simulation results of a group consists of three PUs, (a) operation with group mode transitions, (b) zoomed-in waveforms at time t_1, (c) zoomed-in waveforms at time t_2, (d) zoomed-in waveforms at time t_3, (e) zoomed-in waveforms at time t_4.

is fully charged and is no longer under droop control. In $t_1 - t_2$, BESs of PU2 and PU3 can still absorb surplus power to maintain v_{loc} with droop control to a little higher value due to the higher charging current on each BES. At t_2, BES of PU2 also gets fully charged. In $t_2 - t_3$, solely PU3 BES cannot absorb all the surplus power and is saturated to the maximum charging power. The increase of v_{loc} changes PV converters from MPPT control to droop control which keeps v_{loc} from further increasement, and PVs can evenly share the power. At
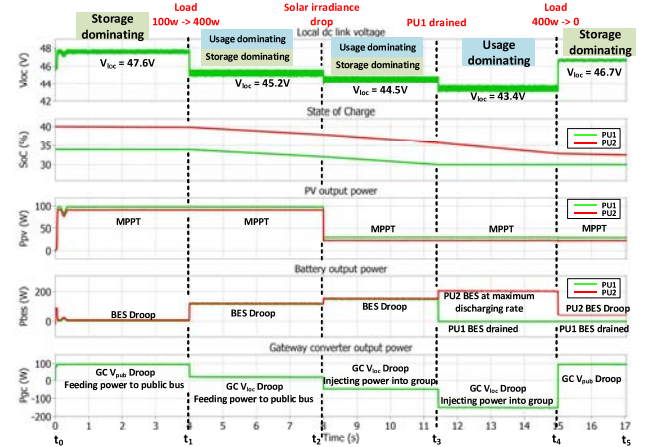

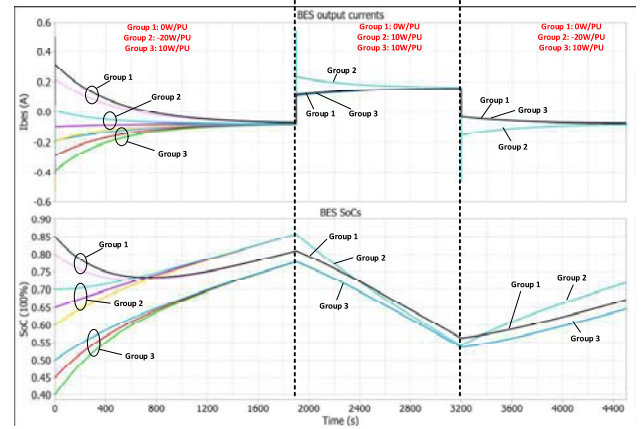Fig. 12. Simulation result of GC mode transitions.

Fig. 13 Simulation result showing power sharing and SoC balance among BESs inside a group and among groups.

t_3, BES of PU3 also gets fully charged. PVs further reduce their output with droop control to maintain v_{loc}. At t_4, a load step change from 100W to 400W happens, that all PVs increase their outputs to MPP still cannot meet the load need. BESs start to discharge and take back droop control.

It can be seen that when BES taking over the droop control, e.g. Fig. 11 (b) and (e), the transient is much faster (shorter settling time and smaller overshoot) than that of PV taking over droop control, e.g. Fig. 11 (c) and (d). It can be explained by that, BES converter uses I-V droop control, as shown in Fig. 4, which has a nature of better transient performance than that of V-I droop control used by PV converter, as shown in Fig. 6 [34]. At the same time, the v_{loc} PI controller of PV converter has to have a lower control bandwidth to guarantee a stable inner v_{PV} loop, which could further deteriorate v_{loc} transient performance. With proper design of parameters and local bus capacitance, the transient can be kept in an accept range as shown in the simulation result (settling time 0.2 s, overshoot 10 V).

Fig. 12 shows the simulation result of a group consists of two PUs and connected to the public bus with a gateway converter GC. The simulation result shows GC operation mode change between v_{pub} control mode and v_{loc} control mode and the case v_{loc} is regulated by both BES and GC. In $t_0 - t_1$, BESs of two PUs are under droop control and PVs are under MPPT

control. GC is working feeding power into public bus of which the power is determined by v_{pub} droop control. At t_1, a load step change from 100W to 400W happens. In $t_1 - t_2$, Both BESs are under droop control with increased output power. Reduced v_{loc} makes GC also under v_{loc} droop control that the power drained from local bus is reduced. At t_2, a solar irradiance drop happens. In $t_2 - t_3$, the v_{loc} is still maintained by BESs and GC. BESs output power are further increased. GC output power is further decreased to negative that start to inject power into local bus. At t_3, PU1 is drained and PU2 BES hits the maximum output power. In $t_3 - t_4$, only GC maintains v_{loc} with droop control. At t_4, the load is reduced to 0 from 400W. v_{loc} rise to a higher value and GC change back to v_{pub} control. PU2 BES maintains v_{loc} while PU1 is still drained that cannot provide any power. Notice that both BES and GC droop control are I-V droop control which has a high control bandwidth. As a result, all transients in Fig. 12 are smooth and fast.

Fig. 13 shows simulation result of a case consists of three groups, where Group 1 has two PUs, Group 2 has three PUs and Group 3 has three PUs. As shown in Fig. 13, all PUs start with different SoC, and net load are different in three groups with two transients of net load step change in Group 2 at 1800s and 3200s. In this test case, the GCs are under v_{pub} control mode to demonstrate power sharing and SoC balancing ability among groups, due to that SoC balancing and power sharing among groups are only considered under GC v_{pub} control mode. Firstly, from the result, with proposed SoC self-convergence control, the SoCs inside a group converges fast to a well-balanced state, as well as the current sharing. Secondly, among multiple groups, as analyzed by mathematical derive from equations (9)-(15), the SoCs of three groups are kept from divergence though with a steady state SoC difference due to different net load/generation condition which agrees to equation (15). And the net load/generation mismatch in different groups are compensated that the BES output powers are well shared by each BES in all groups, with the proposed control design and parameter selection as explained by equation (11).

B. Experiment Verification

The proposed MG architecture has been verified by experimental prototypes, of which the setup is shown in Fig. 14. A MG system with two PUs and one GC converter is tested. The verification focuses more on the group operation. The public bus is emulated as a voltage source with a battery. Each PU is controlled by a TI F28379d DSP. Parameters are set to same as Table II.

Fig. 15 (a) and (b) show the system SoC self-convergence characteristic in charging and discharging process respectively. SoC waveforms are generated by MATLAB with measured information of BES currents. It can be seen that the BES with higher SoC always provides higher current. A converging trend of two BES SoCs can be observed in both cases. Besides that,
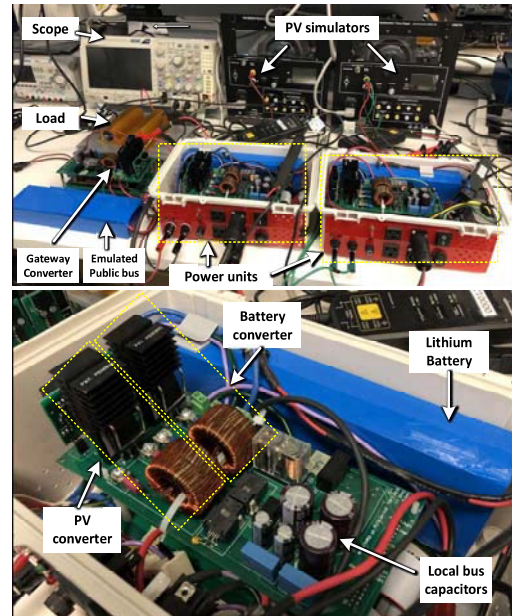

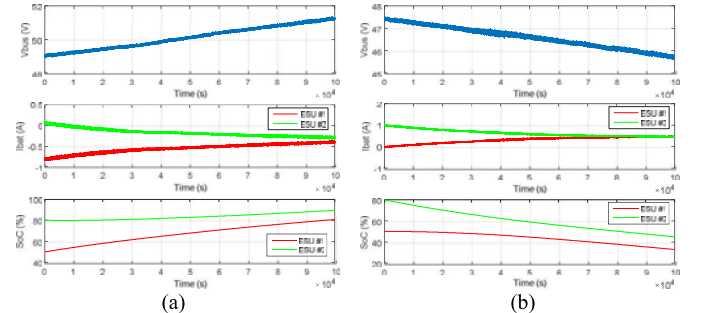Fig. 14. Experiment setup.

| (a) | (b) |

Fig. 15. Experimental waveforms of SoC self-convergence inside a group during (a) charging and (b) discharging.

with change of system overall SoC, a change on the local bus voltage v_{loc} can also be observed, which can be used for GC to estimate local group average SoC.

Fig. 16 shows operation of a standalone PU showing PV-BES droop coordination. In $t_0 - t_1$, BES maintains v_{loc} with droop control and PV operates at MPP. At t_1, BES is fully charged, and BES charging current is saturated to zero; PV converter change to droop control and maintains v_{loc} at a higher level with reduced PV output power. At t_2, solar irradiance is reduced. While PV converter still under droop control, the output power maintains the same but closer to MPP with increased v_{PV}. At t_3, solar irradiance is further reduced. PV converter increases v_{PV} till reach MPP, but the MPP power cannot compensate the load. BES starts to discharge and maintains v_{loc} with droop control. At t_4, solar irradiance is reduced to zero. BES can still maintain v_{loc} with higher output power. Fig. 16 (b) illustrates the operating points of PV during mode transitions.

Fig. 17 shows operation of a group consists of two PUs showing PV-BES droop coordination. Two PV simulators uses different PV curves with different MPP power. In $t_0 - t_1$, PV converters operate at each MPP, and BESs maintain v_{loc} with
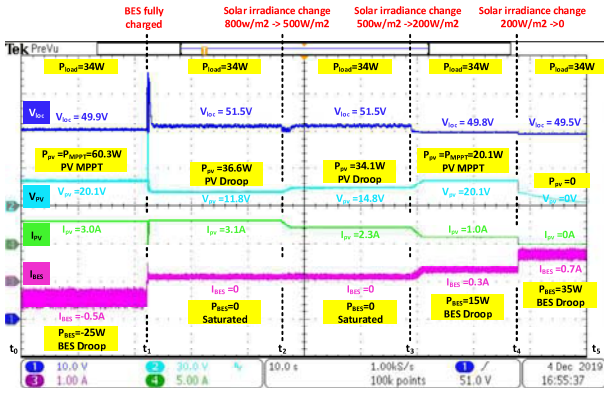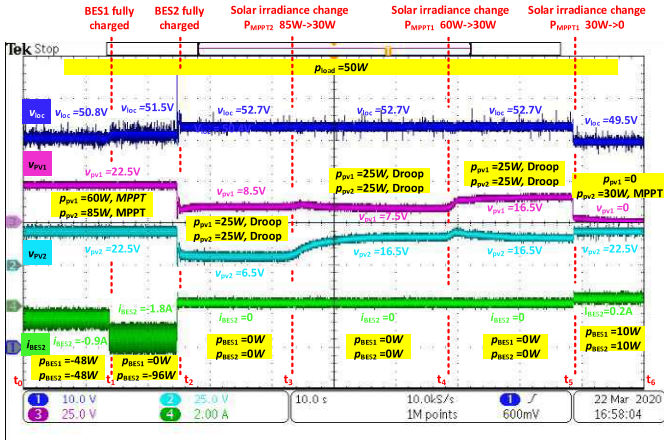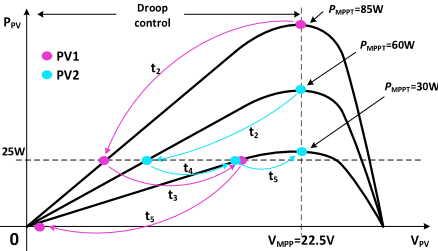
(a)
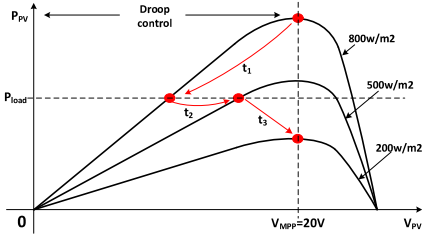
(b)

Fig. 16. Experimental results of a standalone PU showing PV-BES droop control coordination, (a) waveforms, (b) PV operating points.


(a)

(b)

Fig. 17. Experimental waveforms of a group consist of two PUs showing PV-BES droop coordination, (a) waveforms, (b) PV operating points.

droop control and equally share power. At t_1, PU1 BES is fully charged; PU2 BES can still absorb all the surplus power with droop control; PV converters are kept at MPPT control. At t_2, PU2 BES is also fully charged that both BESs cannot absorb any surplus power; PV converters change to droop control. At
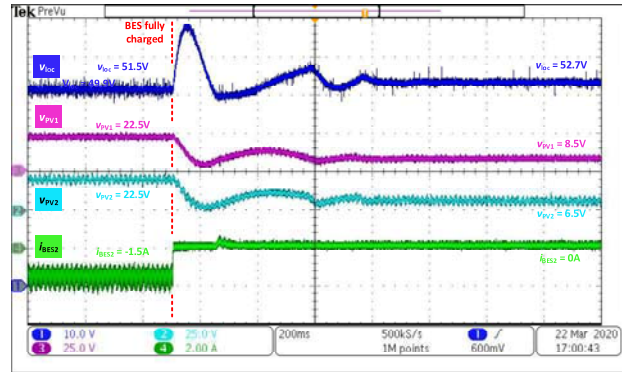
(a)
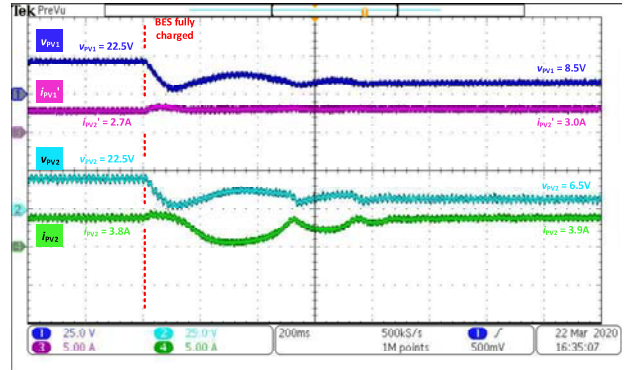
(b)

Fig. 18. Experimental waveforms of transient that both BESs get fully charged and PV converters change to droop control with $P_{load} = 50W$, $P_{MPPT1} = 60W$ and $P_{MPPT2} = 85W$, where (a) shows local bus voltage, PV panel voltages and BES current, and (b) shows PV panel voltages and currents.

t_3, solar irradiance is significantly reduced on PV1, PV converters increase their v_{PV} to maintain the output power. At t_4, solar irradiance is also reduced on PV2, PV converters can still maintain dc link voltage well with equally shared power. At t_5, PV1 is completely shut down, PV2 increase its power till reaching MPP, BESs start to discharge to maintain v_{loc} at lower level with droop control. Fig. 17 (b) shows detailly how the PV operating points move on two different PV curves during the experiment. In storage dominating mode, each PV can track its own MPP. In generation dominating mode, two PVs can equally share the power.

Fig. 18 shows the zoomed in waveforms of the transient from storage dominating mode to generation dominating mode. Fig. 19 shows the zoomed in waveforms of the transient from generation dominating mode back to generation dominating mode. It can be seen the transient of the former one has a much longer settling time and overshoot, due to the nature PV characteristic and V-I droop control. With a proper design of bus capacitance, the overshoot can be limited within an acceptable range.

Fig. 20 shows experimental waveforms of coordination of PU and GC v_{loc} droop control. One PU and one GC is used to verify the BES-GC coordination. Public bus is emulated using a battery as constant voltage source and i_{ref1} is set to 1A. In $t_0 - t_1$, BES with PV output power can well manage the load
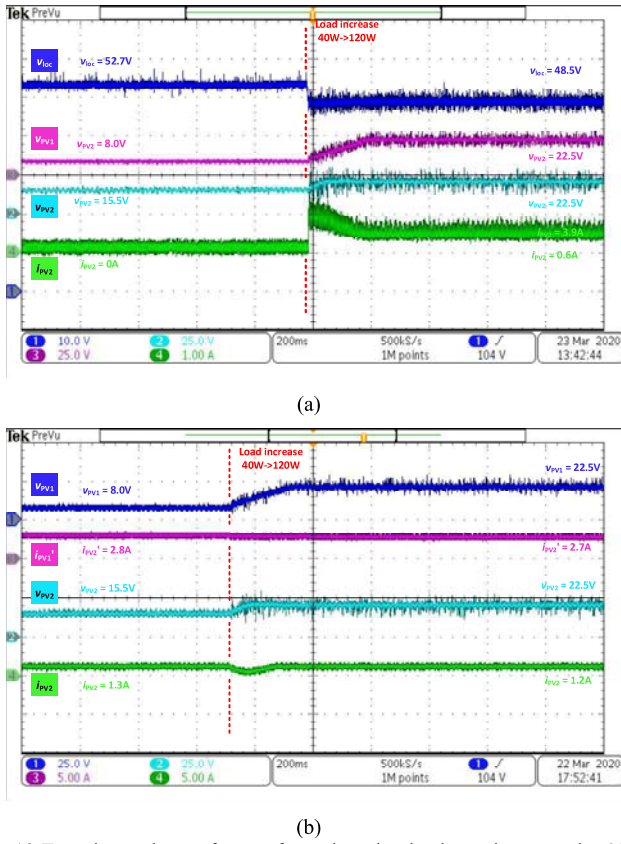
(a)

(b)

Fig. 19 Experimental waveforms of transient that load step increases by $80W$ and PV converters change back to MPPT control with $P_{MPPT1} = 60W$ and $P_{MPPT2} = 25W$, where (a) shows local bus voltage, PV panel voltages and one BES current, and (b) shows PV panel voltages and currents.
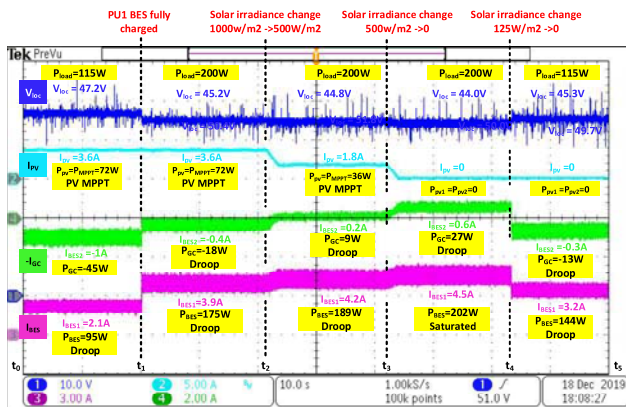

Fig. 20. Experimental waveforms of a PU and a GC showing BES-GC droop coordination.

of 115W maintaining v_{loc} at an acceptable level that GC can injecting 1A as given by reference i_{ref1}. At t_1, load step change to 200W; v_{loc} drops to 45.2V; both BES and GC are under droop control that GC reduces the power injected into public bus to 0.4A. At t_2, solar irradiance change reduces the PV output power; BES increase its output power and GC further reduce its power consumption till injecting power into local group with 0.2A. At t_3, PV output power reduces to zero; BES operates at maximum discharging current; only GC is under

droop control to maintain v_{loc} at a lower level (44V). At t_4, load is reduced to 115W; BES output is reduced and maintains v_{loc} at a relatively higher level with GC.

IV. CONCLUSIONS

In this paper, a module-based Plug-n-Play (PnP) microgrid (MG) is proposed with fully decentralized control. The proposed MG is based on PnP modules namely power units (PU) and gateway converters (GC). Each PU can work as a standalone unit, and with proposed decentralized control technique multiple PUs can be put into a group to scale up the system capacity in an ad-hoc and PnP manner. Groups can be further interconnected through a public bus with gateway converters. Control of each converter just requires local information while power sharing, SoC balancing and mode adaption can be achieved simultaneously in a communication-less manner. The proposed architecture allows people to organically develop power networks in a bottom-up way with PnP modules, which is suitable for electrification in rural areas. The performance of proposed MG and control method are studied analytically and verified by simulation and experimental tests. The results show that, with the proposed method, an ad-hoc low-cost MG with multilayer expandability can be achieved while keeping high reliability and robustness.

REFERENCES

[1] World Energy Outlook, "Energy Access Outlook," 2017. [Online]. Available:https://www.iea.org/publications/freepublications/publication/WEO 2017SpecialReport_EnergyAccessOutlook.pdf.

[2] M. Nasir, H. A. Khan, N. A. Zaffar, J. C. Vasquez and J. M. Guerrero, "Scalable Solar dc Micrigrids: On the Path to Revolutionizing the Electrification Architecture of Developing Communities," *IEEE Electrific. Mag.*, vol. 6, no. 4, pp. 63-72, Dec. 2018.

[3] M. Nasir, H. A. Khan, A. Hussain, L. Mateen and N. A. Zaffar, "Solar PV-Based Scalable DC Microgrid for Rural Electrification in Developing Regions," *IEEE Trans. Sustainable Enery*, vol. 9, no. 1, pp. 390-399, Jan. 2018.

[4] A. Werth, N. Kitamura and K. Tanaka, "Conceptual Study for Open Energy Systems: Distributed Energy Network Using Interconnected DC Nanogrids," *IEEE Trans. Smart Grid*, vol. 6, no. 4, pp. 1621-1630, July 2015.

[5] H. Kakigano, Y. Miura and T. Ise, "Distribution Voltage Control for DC Microgrids Using Fuzzy Control and Gain-Scheduling Technique," *IEEE Trans. Power Electron.*, vol. 28, no. 5, pp. 2246-2258, May 2013.

[6] T. Dragičević, X. Lu, J. C. Vasquez and J. M. Guerrero, "DC Microgrids—Part I: A Review of Control Strategies and Stabilization Techniques," *IEEE Trans. Power Electron.*, vol. 31, no. 7, pp. 4876-4891, July 2016.

[7] A. P. N. Tahim, D. J. Pagano, E. Lenz and V. Stramosk, "Modeling and Stability Analysis of Islanded DC Microgrids Under Droop Control," *IEEE Trans. Power Electron.*, vol. 30, no. 8, pp. 4597-4607, Aug. 2015.

[8] S. Moayedi and A. Davoudi, "Distributed Tertiary Control of DC Microgrid Clusters," *IEEE Trans. Power Electron.*, vol. 31, no. 2, pp. 1717-1733, Feb. 2016, doi: 10.1109/TPEL.2015.2424672.

[9] A. M. Jadhav, N. R. Patne and J. M. Guerrero, "A Novel Approach to Neighborhood Fair Energy Trading in a Distribution Network of Multiple Microgrid Clusters," *IEEE Trans. Ind. Electron.*, vol. 66, no. 2, pp. 1520-1531, Feb. 2019, doi: 10.1109/TIE.2018.2815945.

[10] A. M. Jadhav, N. R. Patne and J. M. Guerrero, "A Novel Approach to Neighborhood Fair Energy Trading in a Distribution Network of Multiple

Microgrid Clusters," *IEEE Trans. Ind. Electron.*, vol. 66, no. 2, pp. 1520-1531, Feb. 2019, doi: 10.1109/TIE.2018.2815945.

[11] Z. Wang, F. Liu, Y. Chen, S. H. Low and S. Mei, "Unified Distributed Control of Stand-Alone DC Microgrids," *IEEE Trans. Smart Grid*, vol. 10, no. 1, pp. 1013-1024, Jan. 2019, doi: 10.1109/TSG.2017.2757498.

[12] C. Tu, F. Xiao, Z. Lan, Q. Guo and Z. Shuai, "Analysis and Control of a Novel Modular-Based Energy Router for DC Microgrid Cluster," *IEEE J. Emerg. Sel. Topics Power Electron.*, vol. 7, no. 1, pp. 331-342, March 2019, doi: 10.1109/JESTPE.2018.2878004.

[13] L. Meng *et al.*, "Review on Control of DC Microgrids and Multiple Microgrid Clusters," *IEEE J. Emerg. Sel. Topics Power Electron.*, vol. 5, no. 3, pp. 928-948, Sept. 2017.

[14] A. Werth *et al.*, "Peer-to-Peer Control System for DC Microgrids," *IEEE Trans. Smart Grid*, vol. 9, no. 4, pp. 3667-3675, July 2018.

[15] V. Nasirian, S. Moayedi, A. Davoudi and F. L. Lewis, "Distributed Cooperative Control of DC Microgrids," *IEEE Trans. Power Electron.*, vol. 30, no. 4, pp. 2288-2303, April 2015.

[16] M. Nasir, Z. Jin, H. A. Khan, N. A. Zaffar, J. C. Vasquez and J. M. Guerrero, "A Decentralized Control Architecture Applied to DC Nanogrid Clusters for Rural Electrification in Developing Regions," *IEEE Trans. Power Electron.*, vol. 34, no. 2, pp. 1773-1785, Feb. 2019.

[17] P. A. Madduri, J. Poon, J. Rosa, M. Podolsky, E. A. Brewer and S. R. Sanders, "Scalable DC Microgrids for Rural Electrification in Emerging Regions," *IEEE J. Emerg. Sel. Topics Power Electron.*, vol. 4, no. 4, pp. 1195-1205, Dec. 2016.

[18] S. Liptak, M. Miranbeigi, S. Kulkarni, R. Jinsiwale and D. Divan, "Self-Organizing NanoGrid (SONG)," *2019 IEEE Decentralized Energy Access Solutions Workshop (DEAS)*, Atlanta, GA, USA, 2019, pp. 206-212.

[19] L. Meng et al., "Flexible System Integration and Advanced Hierarchical Control Architectures in the Microgrid Research Laboratory of Aalborg University," *IEEE Trans. Ind. Appl.*, vol. 52, no. 2, pp. 1736-1749, March-April 2016, doi: 10.1109/TIA.2015.2504472.

[20] Y. Han, X. Ning, P. Yang and L. Xu, "Review of Power Sharing, Voltage Restoration and Stabilization Techniques in Hierarchical Controlled DC Microgrids," in *IEEE Access*, vol. 7, pp. 149202-149223, 2019, doi: 10.1109/ACCESS.2019.2946706.

[21] Q. Shafiee, T. Dragičević, J. C. Vasquez, and J. M. Guerrero, "Hierarchical control for multiple DC-microgrids clusters," *IEEE Trans. Energy Convers.*, vol. 29, no. 4, pp. 922-933, Dec. 2014.

[22] X. Lu, J. M. Guerrero, K. Sun and J. C. Vasquez, "An Improved Droop Control Method for DC Microgrids Based on Low Bandwidth Communication With DC Bus Voltage Restoration and Enhanced Current Sharing Accuracy," *IEEE Trans. Power Electron.*, vol. 29, no. 4, pp. 1800-1812, April 2014, doi: 10.1109/TPEL.2013.2266419.

[23] F. Guo, L. Wang, C. Wen, D. Zhang and Q. Xu, "Distributed Voltage Restoration and Current Sharing Control in Islanded DC Microgrid Systems Without Continuous Communication," *IEEE Trans. Ind. Electron.*, vol. 67, no. 4, pp. 3043-3053, April 2020, doi: 10.1109/TIE.2019.2907507.

[24] Q. Li, F. Chen, M. Chen, J. M. Guerrero and D. Abbott, "Agent-Based Decentralized Control Method for Islanded Microgrids," *IEEE Trans. Smart Grid*, vol. 7, no. 2, pp. 637-649, March 2016, doi: 10.1109/TSG.2015.2422732.

[25] N. L. Diaz, T. Dragičević, J. C. Vasquez and J. M. Guerrero, "Intelligent Distributed Generation and Storage Units for DC Microgrids—A New Concept on Cooperative Control Without Communications Beyond Droop Control," *IEEE Trans. Smart Grid*, vol. 5, no. 5, pp. 2476-2485, Sept. 2014, doi: 10.1109/TSG.2014.2341740.

[26] X. Li *et al.*, "Observer-Based DC Voltage Droop and Current Feed-Forward Control of a DC Microgrid," *IEEE Trans. Smart Grid*, vol. 9, no. 5, pp. 5207-5216, Sept. 2018, doi: 10.1109/TSG.2017.2684178.

[27] M. Mokhtar, M. I. Marei and A. A. El-Sattar, "An Adaptive Droop Control Scheme for DC Microgrids Integrating Sliding Mode Voltage and Current Controlled Boost Converters," *IEEE Trans. Smart Grid*, vol. 10, no. 2, pp. 1685-1693, March 2019, doi: 10.1109/TSG.2017.2776281.

[28] Y. Gu, X. Xiang, W. Li and X. He, "Mode-Adaptive Decentralized Control for Renewable DC Microgrid With Enhanced Reliability and Flexibility," *IEEE Trans. Power Electron.*, vol. 29, no. 9, pp. 5072-5080, Sept. 2014.

[29] K. Sun, L. Zhang, Y. Xing and J. M. Guerrero, "A Distributed Control Strategy Based on DC Bus Signaling for Modular Photovoltaic Generation Systems With Battery Energy Storage," *IEEE Trans. Power Electron.*, vol. 26, no. 10, pp. 3032-3045, Oct. 2011.

[30] X. Lu, K. Sun, J. M. Guerrero, J. C. Vasquez and L. Huang, "Double-Quadrant State-of-Charge-Based Droop Control Method for Distributed Energy Storage Systems in Autonomous DC Microgrids," *IEEE Trans. Smart Grid*, vol. 6, no. 1, pp. 147-157, Jan. 2015.

[31] X. Lu, K. Sun, J. M. Guerrero, J. C. Vasquez and L. Huang, "State-of-Charge Balance Using Adaptive Droop Control for Distributed Energy Storage Systems in DC Microgrid Applications," *IEEE Trans. Ind. Electron.*, vol. 61, no. 6, pp. 2804-2815, June 2014.

[32] A. Elrayyah, Y. Sozer and M. E. Elbuluk, "Modeling and Control Design of Microgrid-Connected PV-Based Sources," *IEEE J. Emerg. Sel. Topics Power Electron.*, vol. 2, no. 4, pp. 907-919, Dec. 2014.

[33] H. Cai, J. Xiang and W. Wei, "Decentralized Coordination Control of Multiple Photovoltaic Sources for DC Bus Voltage Regulating and Power Sharing," *IEEE Trans. Ind. Electron.*, vol. 65, no. 7, pp. 5601-5610, July 2018.

[34] H. Wang, M. Han, R. Han, J. M. Guerrero and J. C. Vasquez, "A Decentralized Current-Sharing Controller Endows Fast Transient Response to Parallel DC–DC Converters," *IEEE Trans. Power Electron.*, vol. 33, no. 5, pp. 4362-4372, May 2018.